

# **Study of Alloy Springs with Magnetorheological Dampers for Vibration Isolator Device**

Dyi-Cheng Chen<sup>\*</sup>, Li-Ren Chen

Department of Industrial Education and Technology, National Changhua University of Education, Changhua 500, Taiwan.

Received 16 July 2017; received in revised form 19 August 2017; accepted 30 August 2017

## **Abstract**

Vibration is a factor that must be controlled during the manufacturing process; variation in workpiece dimensions often results in inaccuracies due to vibration. This study adopted a spring and electromagnetic-repulsion and magnetorheological damper that can absorb the energy of external vibrations and deduced the influential vibration factors. ANSYS was employed to determine the energy that could be absorbed by the vibration isolation device under machine vibration, and the Taguchi method of quality engineering was used to design the structure of the device (metal spring, wire diameter, and material). The usability of the product was examined for application in computer numerical control and traditional machines. The considered parameters of the magnetorheological fluid were density, coefficient of elasticity, and Poisson's ratio. The results indicated that spring wire diameter exerted the strongest effect on the device's performance and that the electrical current provided to the damper could be buffered.

**Keywords:** vibration isolation device, alloy springs, magnetorheological dampers

## **1. Introduction**

Serving as a semiactive control element, a magnetorheological (MR) damper is a smart damping device that is controlled by a magnetic field [1]. An MR damper with semiactive control integrated with the controllability and flexibility of active damping can adjust its damping force in response to load force and structure and is characterized by passive stability and energy conservation. The dynamics of an MR damper under different input voltages [2] enable the input voltage to pass through a current driver, which generates an electric current. The electric current then passes through a coil to generate a magnetic field; adjusting the input voltage thus changes the magnetic field strength.

Kim et al. [3] proposed an innovative friction pendulum system and MR damper that utilize the isolator and auxiliary damper of a smart base isolation system. A fuzzy logic controller is generally used to regulate an MR damper because it has inherent robustness and its capability in processing nonlinear and uncertainty data. Beijen et al. [4] demonstrated that a control scheme with two sensors was superior that with sensor fusion because cyclic shaping and greater stability are possible. Van der Sandea et al. [5] proposed that by changing the weighting filter, different controllers could be designed to emphasize comfort or controllability.

## **2. Research Methods**

### *2.1. Simulation analysis of the organization*

SolidWorks was used to design the vibration isolation device and mechanism shown in Fig. 5. The overall design concept of the mechanism is displayed in Figs. 1 and 2. During an earthquake, the springs absorb vibration. Because earthquake movement can occur in various directions—for example, horizontal or vertical—this mechanism was designed to enable absorption regardless of the direction of movement.

---

<sup>\*</sup> Corresponding author. Email address: dcchen@cc.ncue.edu.tw

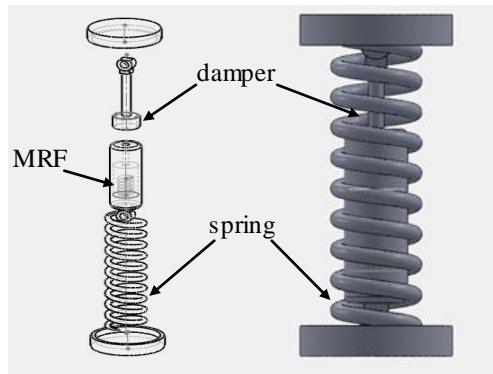


Fig. 1 Vibration isolation device

## 2.2. ANSYS

ANSYS is a finite element analysis software package; its processing operations can be divided into a preprocessor, postprocessor, and solver. The postprocessor module displays calculated results using graphical methods such as a color contour, gradient, vector, particle track, three-dimensional section, transparent, and semitransparent displays. Calculated results can be displayed or output in the forms of charts or curves.

## 2.3. Taguchi quality engineering

The offline quality control of Taguchi employs three-stage quality engineering design to achieve a robust product. In the first stage, which is system design, engineering personnel determine the ideal product design concepts according to their professional knowledge, experience, and mutual discussion. In the second stage, parameter design, relevant process parameters are selected and an orthogonal arrangement is used to conduct an experiment, the purpose of the orthogonal arrangement is to reduce the sensitivity of the product toward interference by noise and thus reduce variation in product quality. The third stage, tolerance design, focuses on process operating conditions and analyzes causes of product variation to determine the product's tolerance range. The loss function can be used to calculate product cost after the tolerance design stage. Loss functions are used in quality engineering to obtain a balance between cost and quality. This research project employed an orthogonal array (OA) to plan the experiment. The response table and factor effect diagram were used to determine the effect of each factor on a target value and then to select the most favorable parameter combination.

## 3. Results of Research and Analysis

### 3.1. The setting of magnetorheological fluid

Prior to simulation analysis, the parameters of the MR fluid (MRF) had to be set, including its density, coefficient of elasticity, and Poisson's ratio. The Poisson's ratio of a fluid is 0.5. In consideration of the changes to the MRF under different magnetic currents, the Poisson's ratio of the MRF was set at that of rubber (i.e., 0.45).

The density of magnetorheological fluids is known from the description of Lord's magnetorheological damper products. The elastic modulus of the parameters set for the magnetorheological fluid is required to complex modulus  $G^*$ , the modulus of the modulus of the material show the relationship between the stress-strain ratio, the modulus of the complex modulus  $G^*$

$$G^* = G' + iG'' \quad (1)$$

$G'$  is Young's coefficient of storage modulus, and the viscoelastic material by the vibration of the storage energy elastic part.  $G''$  for the loss modulus is the viscoelastic material by the vibration force when the part of the energy consumption. Sun et al. [6] obtained experimental data to obtain a set of non-linear relationship between the modulus and loss modulus of the magnetorheological material and the magnetic field:

$$G' = 3.11 \times 10^{-7} B^2 + 3.56 \times 10^{-4} B + 5.78 \times 10^{-1} \tag{2}$$

$$G'' = 3.47 \times 10^{-9} B^2 + 3.85 \times 10^{-6} B + 6.31 \times 10^{-3} \tag{3}$$

B is the magnetic induction intensity, unit mT.

Different magnetic fields result in different magnetic induction intensities, as illustrated in Fig. 15. The magnetic induction intensity was substituted into (1) to obtain the complex modulus  $G^*$ , which is detailed in Table 1.

Table 1 MRF-140CG magnetorheological damper parameters

current	Magnetic induction (mT)	G'(MPa)	G''(MPa)	G*(MPa)
0	0	0.578	0.006	0.578+0.006i
0.5	350	0.74	0.008	0.74+0.008i
1	550	0.867	0.009	0.867+0.009i

3.2. The setting of magnetorheological fluid

Table 2 displays the settings of various material parameters. The force exerted above the shock absorber mechanism during each simulation was 5000 N; pressure was applied downward, and the total deformation and von Mises stress were determined.

Table 2 Material parameters table

material	Al	JIS G 3522	Si-Cr Alloy	SUS316	MRF-140CG
density (g/cm <sup>3</sup> )	2.7	7.85	7.86	8.02	3.64
Young's modulus (MPa)	69000	205882	207000	186274	1.03
Poisson's ratio	0.34	0.3	0.3	0.3	0.45

3.3. Application of Taguchi method to be optimized

This study select four spring factors and one MRF factor for the vibration isolation device (Table 3). Table 4 lists the  $L_{27}(3^5)$  OA comprising the total deformation and von Mises stress obtained through 27 simulations with various parameter values.

Table 3 Earthquake device mechanism parameter factor

	A	B	C	D	E
<b>Factor</b>	Wire diameter (mm)	Spring center diameter (mm)	Space(mm)	Spring material	Current(A)
Level 1	6	50	20	JIS G 3522	0
Level 2	8	60	25	Si-Cr Alloy	0.5
Level 3	10	70	30	SUS316	1

Table 4 L 27(35)

	A	B	C	D	E	Total Deformation	von Mises stress	TD S/N	vMs S/N
1	1	1	1	1	1	0.13853	96.240	17.1691	-39.6671
2	1	1	1	1	2	0.13853	96.240	17.1691	-39.6671
3	1	1	1	1	3	0.13853	96.240	17.1691	-39.6671
4	1	2	2	2	1	0.04635	99.377	26.6790	-39.9457
5	1	2	2	2	2	0.04635	99.377	26.6790	-39.9457
6	1	2	2	2	3	0.04635	99.377	26.6790	-39.9457
7	1	3	3	3	1	0.13844	96.858	17.1748	-39.7227
8	1	3	3	3	2	0.13844	96.858	17.1748	-39.7227
9	1	3	3	3	3	0.13844	96.858	17.1748	-39.7227
10	2	1	2	3	1	0.15817	96.500	16.0175	-39.6905
11	2	1	2	3	2	0.15817	96.500	16.0175	-39.6905
12	2	1	2	3	3	0.15817	96.500	16.0175	-39.6905
13	2	2	3	1	1	0.14809	206.540	16.5895	-46.3001
14	2	2	3	1	2	0.14809	206.540	16.5895	-46.3001
15	2	2	3	1	3	0.14809	206.540	16.5895	-46.3001
16	2	3	1	2	1	0.14757	96.786	16.6200	-39.7163
17	2	3	1	2	2	0.14757	96.786	16.6200	-39.7163
18	2	3	1	2	3	0.14757	96.786	16.6200	-39.7163
19	3	1	3	2	1	0.15206	95.335	16.3597	-39.5850
20	3	1	3	2	2	0.15206	95.335	16.3597	-39.5850
21	3	1	3	2	3	0.15206	95.335	16.3597	-39.5850
22	3	2	1	3	1	0.16921	97.125	15.4315	-39.7466
23	3	2	1	3	2	0.16921	97.125	15.4315	-39.7466
24	3	2	1	3	3	0.16921	97.125	15.4315	-39.7466
25	3	3	2	1	1	0.15234	96.001	16.3437	-39.6455
26	3	3	2	1	2	0.15234	96.001	16.3437	-39.6455
27	3	3	2	1	3	0.15234	96.001	16.3437	-39.6455

As shown in Tables 5 and 6, the most favorable parameters obtained for four factors at three levels were a spring wire diameter of 6 mm (A1), spring center diameter of 60 mm (B2), spring coil spacing of 25 mm (C2), spring material of chrome silicon (D2), and damper current of 0 A (E). Regarding the degree of importance to the vibration isolation mechanism, the parameters were in a descending order of spring wire diameter > spring material > spring coil spacing > spring center diameter > damper current. Fig. 3 plots the S/N (smaller) factor response of the total deformation.

Table 5 Total Deformation S / N ratio factor reaction

Level	A	B	C	D	E
1	20.34	16.52	16.41	16.70	17.60
2	16.41	19.57	19.68	19.89	17.60
3	16.04	16.71	16.71	16.21	17.60
Delta	4.30	3.05	3.27	3.68	0.00
Rank	1	4	3	2	5

Table 6 Total Deformation of the best parameters

A1	B2	C2	D2	E
Wire diameter (mm)	spring center diameter (mm)	Space(mm)	Spring material	Current(A)
6	60	25	Si-Cr Alloy	0

The most favorable obtained parameters were used to construct a model, and ANSYS analysis was performed to obtain the following results: greatest total deformation of 0.169 mm (Fig. 4 (a)) and greatest von Mises stress of 97.12 MPa (Fig. 4 (b)).

As shown in Tables 7 and 8, the most favorable parameters obtained for the four factors at the three levels were a spring wire diameter of 10 mm (A3), spring center diameter of 50 mm (B1), spring coil spacing of 20 mm (C1), spring material of SUS316 (D3), and damper current of 0 A (E). The parameters had the following order of importance in their effect on the vibration isolation mechanism: spring center diameter > spring wire diameter > spring coil spacing > spring material > damper current. Fig. 5 shows the S/N (smaller) factor response diagram of von Mises stress.

Table 7 von Mises S / N ratio factor reaction

Level	A	B	C	D	E
1	-39.78	-39.65	-39.71	-41.87	-40.45
2	-41.90	-42.00	-39.76	-39.75	-40.45
3	-39.66	-39.69	-41.87	-39.72	-40.45
Delta	2.24	2.35	2.16	2.15	0.00
Rank	2	1	3	4	5

Table 8 Von Mises of the best parameters

A3	B1	C1	D3	E
Wire diameter (mm)	spring center diameter (mm)	Space(mm)	Spring material	Current(A)
10	50	20	SUS316	0

The most favorable obtained parameters were used to construct a model, and ANSYS analysis was performed to determine the greatest total deformation of 0.166 m (Fig. 6 (a)) and greatest von Mises stress of 97.38 GPa (Fig. 6(b)).

#### 4. Conclusions

In this study, the investigated MRF was treated similar to a solid to configure the material parameters. During the simulation process, these parameters were simplified by overlooking viscosity. Optimal values of total deformation and von Mises stress were obtained through simulation analysis followed by Taguchi analysis. Quality characteristics were selected based on the smaller the better situation to minimize product variation. The optimal parameter results obtained through simulation analysis revealed that spring wire diameter had the most crucial effect on the performance of the vibration isolation mechanism; increasing the spring wire diameter would increase the seismic performance of the mechanism. Proper selection of the spring center diameter and spring coil spacing also enhances seismic performance. The results of this study can serve as a useful reference for relevant industry.

**Typical Magnetic Properties**

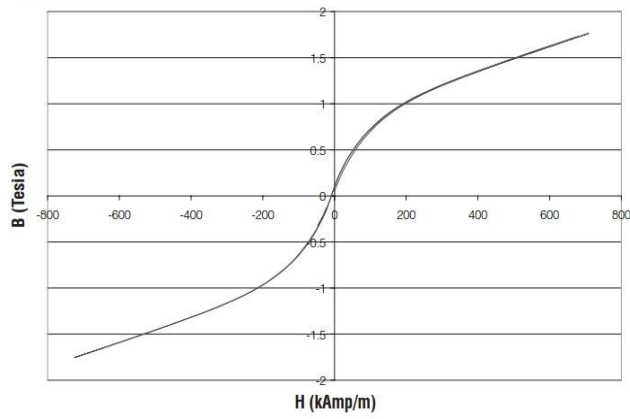


Fig. 2 MRF-140CG magnetorheological damper magnetic field and magnetic induction change map

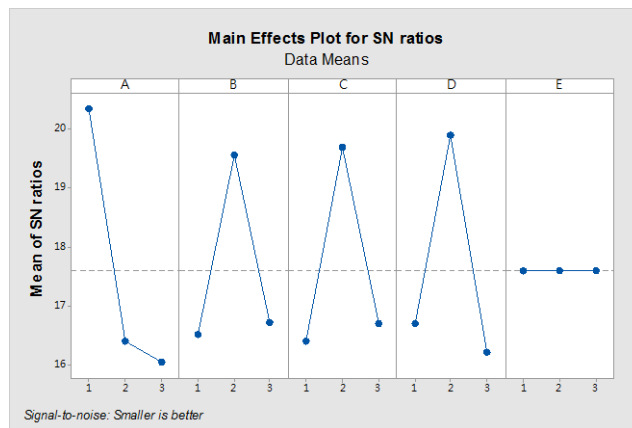
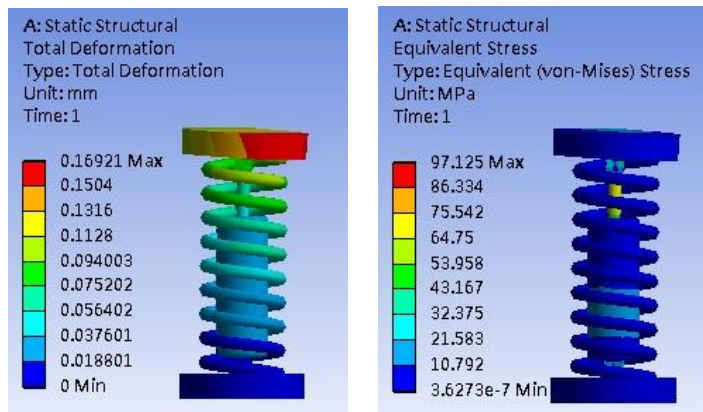


Fig. 3 Total deformation S / N ratio calculation



(a) Total deformation

(b) Von Mises stress

Fig. 4 Total deformation model and von Mises stress

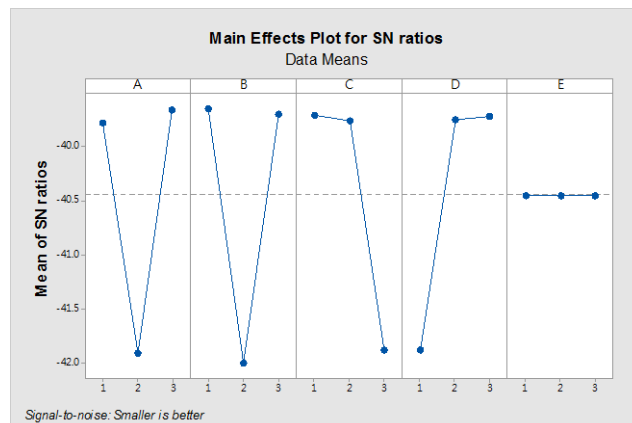


Fig. 5 Von Mises stress S / N ratio calculation

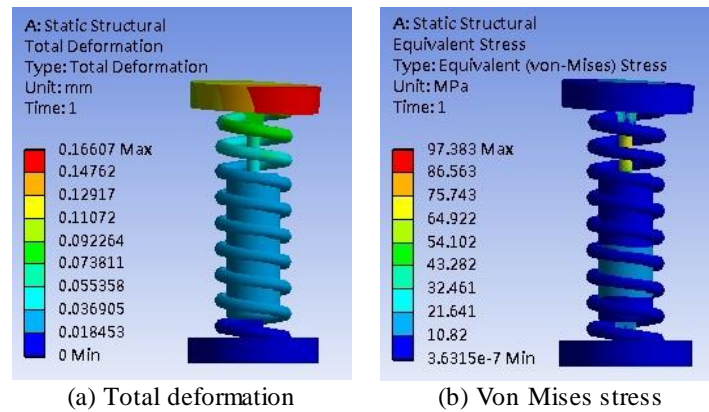


Fig. 6 Total deformation model and von Mises stress

## References

- [1] S. Narasimhan, S. Nagarajaiah, and E. A. Johnson, "Smart base-isolated benchmark building part IV: Phase II sample controllers for nonlinear isolation systems," *Structural Control and Health Monitoring*, vol. 15, no. 5, pp. 657-672, July 2008.
- [2] S. J. Dyke, B. F. Spencer Jr., M. K. Sain, and J. D. Carlson, "Modeling and control of magnetorheological dampers for seismic response reduction," *Smart Materials and Structures*, vol. 5, no. 5, pp. 565-575, 1996.
- [3] H. S. Kim and P. N. Roschke, "Design of fuzzy logic controller for smart base isolation system using genetic algorithm," *Engineering Structures*, vol. 28, no. 1, pp. 84-96, January 2006
- [4] M. A. Beijen, D. Tjepkema, and J. van Dijke, "Two-sensor control in active vibration isolation using hard mounts," *Control Engineering Practice*, vol. 26, pp. 82-90, May 2014.
- [5] T. P. J. van der Sandea, B. L. J. Gysenb, I. J. M. Besselinka, J. J. H. Paulides, E. A. Lomonova, and H. Nijmeijer, "Robust control of an electromagnetic active suspension system: Simulations and measurements," *Mechatronics*, vol. 23, no. 2, pp. 204-212, May 2013.
- [6] Q. Sun, J. X. Zhou, and L. Zhang, "An adaptive beam model and dynamic characteristics of magnetorheological materials," *Journal of Sound and Vibration*, vol. 261, no. 3, pp. 465-481, March 2003.